A spallation target at TRIUMF for fundamental neutron physics

Sean Vanbergen[1,2*], *Wolfgang* Schreyer[1], *Shomi* Ahmed[3], *Taraneh* Andalib[3], *Mike* Barnes[4], *Beryl* Bell[1,5], *Jason* Chak[1], *Elspeth* Cudmore[1,6], *Beatrice* Franke[1,2], *Pietro* Giampa[1], *Patricia* Gnyp[1,7], *Moritz* Hahn[7], *Sean* Hansen-Romu[3], *Kichiji* Hatanaka[8], *David* Jones[2], *Katerina* Katsika[1], *Shinsuke* Kawasaki[9], *Elie* Korkmaz[10], *Kirk* Madison[2], *Juliette* Mammei[3], *Russell* Mammei[1,3,11], *Cameron* Marshall[1], *Jeffery* Martin[1,11], *Ryohei* Matsumiya[1,8], *Kenji* Mishima[9,12], *Takahiro* Okamura[9], *Ruediger* Picker[1], *Edgard* Pierre[1], *Des* Ramsay[1], *Gelo* Remon[1], *Steve* Sidhu[1,13], *Brendan* Thorsteinson[11], and *Willem* van Oers[1]

[1]TRIUMF, Vancouver, BC, Canada
[2]University of British Columbia, Vancouver, BC, Canada
[3]University of Manitoba, Winnipeg, MB, Canada
[4]Center for European Nuclear Research, CH-1211 Geneva 23, Switzerland
[5]McGill University, Montreal, QC, Canada
[6]Carleton University, Ottawa, ON, Canada
[7]Coburg University of Applied Science, Coburg, Germany
[8]Research Center for Nuclear Physics, Osaka University, Ibaraki, Osaka, Japan
[9]High Energy Accelerator Research Organization, KEK, Tsukuba, Ibaraki, Japan
[10]University of Northern British Columbia, Prince George, BC, Canada
[11]University of Winnipeg, Winnipeg, MB, Canada
[12]J-PARC, Tokai, Ibaraki, Japan
[13]Simon Fraser University, Burnaby, BC, Canada

Abstract. Ultracold neutrons (UCNs) are a powerful tool for probing the Standard Model at high precision. The TRIUMF Ultracold Advanced Neutron (TUCAN) collaboration is building a new UCN source to provide unprecedented densities of UCNs for experiments. This source will use a tantalum-clad tungsten spallation target, receiving up to 40 μA of 480-MeV protons from TRIUMF's main cyclotron. The beamline and target were constructed from 2014 to 2016 and operated at beam currents up to 10 μA from 2017 to 2019 as part of a prototype UCN source. We describe the design choices for the target and target-handling system, as well as our benchmarking of the target performance using UCN production measurements.

1 Introduction

Ultracold neutrons (UCNs) are neutrons with kinetic energies less than the optical Fermi potential of certain solid materials, with the upper cut-off corresponding to the potential of Ni-58 at 347 neV. Fulfilling this energy condition allows UCNs to be reflected from material surfaces under any angle of incidence, and so they can be contained and studied for hundreds of seconds.

This containment property has made UCNs a powerful tool for probing fundamental physics and testing extensions of the standard model. Measurements of the neutron lifetime and beta decay asymmetry test the weak interaction, including unitarity of the CKM matrix [1]. Searches for electric dipole moments [2] are a precise test of CP violation and can help explain the observed matter-antimatter asymmetry in the universe [3, 4]. UCNs also provide a rare system where gravity can be observed in a quantum-mechanical context and allow non-Newtonian gravity to be tested [5, 6].

Improving the precision of such experiments requires achieving higher UCN densities in experimental apparatuses. Modern UCN sources are based on the conversion of cold neutrons to UCNs through interactions with fundamental excitations (phonons and rotons) in bulk materials. This process is non-conservative and can therefore produce high phase-space densities, enabling similarly high real-space densities in experiments. UCN sources utilizing this technique have been developed using solid D_2 [8-11] and superfluid He-II [12-14].

At TRIUMF, the TUCAN collaboration is building a new UCN source, using room-temperature D_2O and 20 K D_2 neutron moderators to produce cold neutrons and He-II as a UCN converter [15]. This source will achieve a world-class UCN density and enable a new generation of high-precision neutron experiments [16].

Neutron production in the TUCAN source is achieved by spallation. A new 480-MeV proton beamline, driven by the TRIUMF main cyclotron, has been constructed for this purpose, which we have described in previous publications [17]. In these proceedings, we describe the details of the target design, handling, and analysis of its performance.

* Corresponding author: svanbergen@triumf.ca

2 Target design

The TUCAN source target, shown in Fig. 1, is a set of five tantalum-clad water-cooled tungsten blocks, enclosed in a stainless-steel flask through which the cooling water circulates.

Tungsten has long been considered an ideal material for the construction of solid spallation targets due to its high neutron yield and high strength at elevated temperatures. The choice of tungsten as a target material was driven by the successful design of such a target for the now-decommissioned KENS facility [18]. Targets of a similar composition have continued to operate with great success at LANSCE [19] and ISIS [20]. Tungsten targets will also be used the ESS, although with a substantially different design [21].

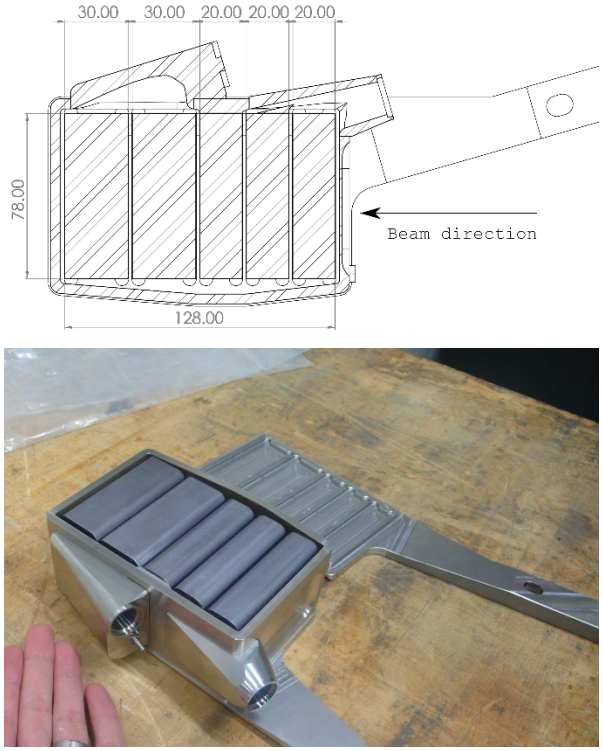

Fig. 1. Top: schematic of the target blocks, showing the dimensions of the blocks in mm. The height of the blocks, not shown, is 56 mm. Bottom: photograph of the target flask with the blocks inside. The inlet (front) and outlet (rear) of the flask are visible in the bottom left corner.

The limitation of tungsten as a target material is that it experiences a high rate of corrosion in water under high temperature or radiation. The solution to this has been to clad tungsten targets with a second material that is resistant to corrosion [18]. Tantalum has been studied as an ideal material for this cladding, as it also has a high neutron yield. A 0.86-mm-thick tantalum cladding was applied to the TUCAN target blocks using hot isostatic pressing (HIP). This process was performed by Allied Materials Inc. at a temperature of 1500 °C and a pressure of 200 MPa in high-purity (5N) argon.

At the maximum current of 40 μA and a typical proton energy of 480 MeV, the beam will deliver approximately 20 kW to the target. Simulations of the spallation process using MCNP [22] indicate that 70% of the energy is deposited as heating of the target, with the remaining 30% being carried away by the spallation products. The energy deposited in the target is removed by a convective water-cooling loop.

The target geometry has been optimized alongside the water-cooling to reduce heating and stress. A total target thickness of 12 cm was chosen such that all protons are stopped in the target. A single 12-cm-thick block would experience un-manageable heating, and so it is necessary to split the target into several blocks.

Extensive finite element simulations of the target heating and water cooling were carried out using ANSYS to determine a suitable geometry, an example of which is shown in Fig. 2. These studies explored different numbers of blocks and different block thicknesses to arrive at the chosen geometry, shown in figure 1. This geometry consists of five blocks, with the first three being 20 mm thick, and the last two being 30 mm thick. The blocks are separated by 2 mm wide channels through which the cooling water circulates with a total flow rate of 0.75-0.9 kg/s at 70 psig supply pressure.

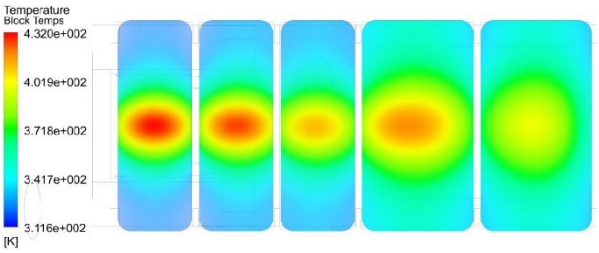

Fig. 2. Finite-element simulated temperature profiles in the target blocks from heating by the 40-μA 480-MeV proton beam. The profiles are cut through the centre of the blocks, corresponding to the centre of the beam where maximum heating occurs.

Table 1. Maximum stresses and temperatures achieved in different parts of the target.

Location	Maximum Stress (MPa)	Maximum Temperature (°C)
Target blocks	96	158
Flask window	88	72
Cooling water	N/A	119

The resulting maximum temperatures and stresses in the target are shown in Table. 1. The steel of the flask has a yield strength of 205 MPa. The cooling water should be kept below its boiling point, which at the pressure of the water supply is 158 °C. Both conditions are satisfied by the design.

Design parameters for the target were originally chosen based on the experience of the KENS target, which indicated that the temperature gradient in each block should be kept below 200 °C, and the stress below 200 MPa [23].

Due to the higher beam current compared to KENS (which was operated up to 10 μA), the target may see faster loss of strength due to irradiation damage. From FLUKA [24,25] simulations, the target is expected to see a maximum 1.1 dpa and 118 He appm per year. Recent studies have characterized the effect of such levels of irradiation damage on tungsten and tantalum [26]. Based on these results, the target's ultimate

strength should remain above 200 MPa after 10 years of operation, after which the target will be replaced.

3 Target handling system

The target is inserted into a helium-filled aluminium crypt at the end of the proton beamline. The crypt is separated from the vacuum beam pipe by a 1-mm-thick Al-2219 window. This material was chosen due to its superior strength at high temperature, as simulations of the window indicate that it could reach up to 120°C during operation. The purpose of the crypt is to provide a separating region between the target and the rest of the beamline, especially in the event of any damage to the target such as a cooling-water leak. The helium atmosphere provides some additional cooling of the crypt while not being significantly activated by the beam.

The target is held in the crypt by the target arm, shown in Fig. 3. The arm is built in three sections: the fore-arm, the mid-arm, and the carriage. The fore-arm directly connects to the target flask, and is connected to the mid-arm with a special disconnection joint. This joint allows the fore-arm, with the target flask, to be disconnected for disposal. The mid-arm connects the fore-arm and the carriage. The carriage is a large steel block that provides a counterweight to support the cantilever of the arm and serves as shielding against prompt radiation from the target. It also serves as part of the target extraction system.

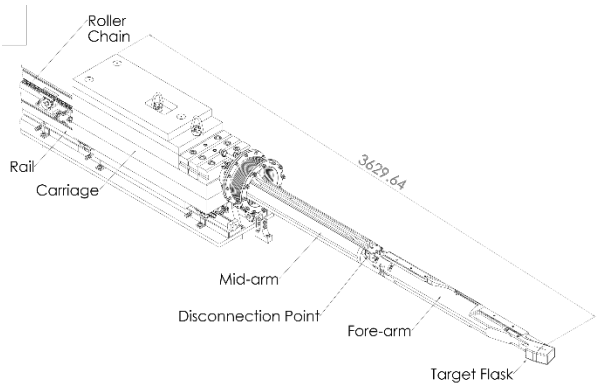

Fig. 3. The target arm, consisting of the fore-arm, mid-arm, and carriage, which together support the target in the beamline. The carriage rests on a pair of rails, and is connected via a roller chain to a gearbox (not shown) which is used to move the target arm into and out of the beamline.

The extraction system is formed by a set of hardened-steel rails on which the carriage rests. At the end of the rails is a gearbox, connected to the carriage by a roller chain. During manoeuvring of the target, the gearbox is driven by a long pole, allowing the target to be moved without exposure to high dose rates.

The target extraction has been designed with a minimum target life of 10 years. After reaching end of life, the target must be removed and stored. At this point, the target will be heavily irradiated and must be placed in long-term shielded storage. For that purpose, a lead-lined storage cask has been built.

The target cask was developed using FLUKA simulations to determine the dose rate. After operating the target for 20 years with an average beam current of 10 μA (a 25% duty cycle on the 40 μA beam current) the equivalent-dose rates close to the target can exceed 1 Sv/h. Extraction of the target requires removal of concrete shielding, which is only possible during the yearly 3-months-long shutdown of the TRIUMF cyclotron. During this time, short-lived radionuclides will be allowed to decay for a cooldown period of approximately one month. Then the target will be extracted and placed in the cask. Fig. 4 shows the equivalent-dose rate at 50 cm from the target cask as a function of cooldown time. After a 28-day cooldown period, the equivalent-dose rate is reduced below 200 μSv/h, allowing the cask to be safely handled by trained personnel and transported to a long-term storage location.

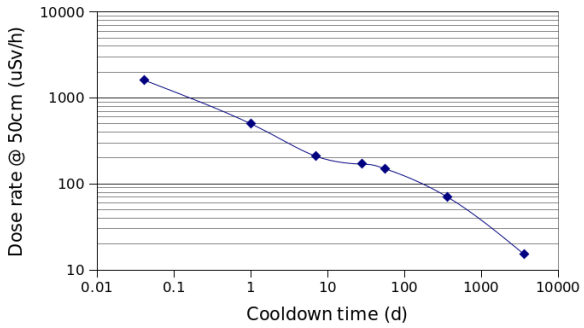

Fig. 4. Equivalent-dose rate, calculated using FLUKA, at 50 cm distance from the target cask, once the target has been placed in the cask, following 20 years of operation and a cooldown period to allow short-lived radionuclides to decay.

4 Performance benchmarking

The performance of the target has been tested by comparing simulation results to measurements of UCN production.

In 2017, we installed a prototype UCN source, which was originally developed and operated at RCNP Japan [27], above the spallation target. This source used He-II as a UCN converter, but with a significantly lower cooling power compared to the new TUCAN source, which limited the operation current. This source used graphite, heavy water, and heavy-water ice cooled to 20 K to moderate the fast spallation neutrons to cold neutrons. The cold neutrons were then converted to UCNs in an 8-litre volume of He-II cooled to 1 K. The geometry of this source relative to the target are described in detail in our previous publication [28].

During 2017, 2018, and 2019 we operated the beamline, spallation target, and UCN source for a month each year [28]. During these experimental campaigns, measurements were made to understand the production of UCN by the source. For such a measurement, we typically irradiated the target for 60 s while a valve confined the UCN inside the source. Then, the valve was opened and the UCN accumulated in the source diffused along stainless-steel guides to a detector.

A fast kicker magnet installed in the beamline [29] allows us to vary the average beam current diverted to

the target. Fig. 5 shows the expected linear proportionality between beam current and UCN counted in the detector up to 1 μA. We have operated the beamline at higher currents, up to 10 μA, but due to limited cooling power to maintain the He-II temperature, the prototype UCN source was not able to handle the increased heat loads at higher currents. This causes us to observe a decrease in the UCN yield.

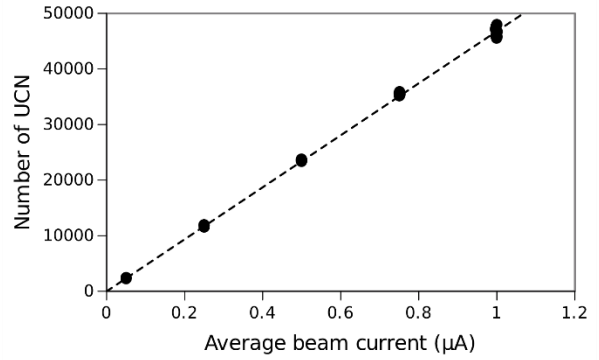

Fig. 5. UCN extracted from the source after irradiating the target with varying average beam currents for 60 s. The UCN yield increases linearly with current up to 1 μA [17, 28]. The larger scatter in the points at 1 μA can be attributed to fluctuations in the source conditions.

To understand the neutron production, we modelled the target, moderators, and UCN source in MCNP [22], shown in fig. 6. The UCN production rate in the prototype source expected from these simulations was 21000 $s^{-1}\mu A^{-1}$. This number was used as an input for UCN Monte Carlo transport simulations using PENTrack [30]. The results of these simulations showed good agreement with the detected number of 42000 UCNs at 1 μA beam current [28].

In this analysis, there were significant uncertainties in the transport properties of UCN guides and in temperature-dependent UCN losses inside the source, which resulted in equally large uncertainties on the exact performance parameters of the source. Despite these limitations, the results are consistent with the target operating as expected.

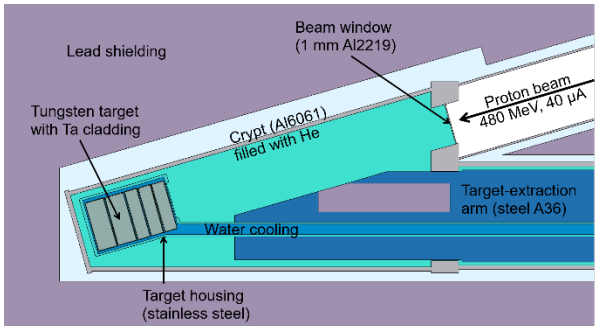

Fig. 6. Simulation model of the target (top view) [27, 31].

5 Conclusion

We have developed and installed a tantalum-clad tungsten spallation target as part of the TUCAN source. This target has been designed to accept 40 μA of 480 MeV proton beam current with an expected operational lifetime of 10-20 years. All target handling systems have been completed and the target is ready for long-term operation. The target performance has been operated at currents up to 10 μA. UCN production data up to 1 μA has been analysed and found to be consistent with the expected source performance.

Beginning in 2024, the target will be operated as part of the new TUCAN source at currents up to 40 μA. Based on our predictions of the source performance [16], we expect the TUCAN source to be capable of producing the highest density of UCN in experiments ever achieved. This will enable a new generation of high-precision experiments using neutrons.

References

1. D. Dubbers and B. Markisch, Annu. Rev. Nucl. Part. 71, 139-163 (2021)
2. J. W. Martin J. Phys.: Conf. Ser. 1643, 012002 (2020)
3. V. Cirigliano, Y. Li, S. Profumo, and M. J. Ramsey-Musolf, J. High Energy Phys. 2010 (2010)
4. S. J. Huber, M. Pospelov, and A. Ritz, Phys. Rev. D 75, 036006 (2007).
5. R. I. Sedmik, J. Bosina, L. Achatz, et. al., EPJ Web Conf. 219, 05004 (2019).
6. B. Clement, S. Baeßler, V. V. Nesvizhevsky, et. al., arXiv:2205.11130 (2022).
7. T. Jenke, G. Cronenberg, J. Burgdorfer, et. al., Phys. Rev. Lett. 112, 151105 (2014)
8. T. M. Ito, E. R. Adamek, N. B. Callahan, et. al., Phys. Rev. C 97, 012501 (2018).
9. J. Kahlenberg, D. Ries, K. U. Ross, et. al., Eur. Phys. A 53 (2017)
10. B. Lauss and B. Blau, SciPost Phys. Proc. 004 (2021).
11. E. Korobkina, G. Medlin, B. Wehring, et. al., NIM A 767, 169 (2014)
12. F. M. Piegsa, M. Fertl, S. N. Ivanov, et. al., Phys. Rev. C 90, 015501 (2014).
13. Y. Masuda, K. Hatanaka, S.-C. Jeong, et. al., Phys. Rev. Lett. 108, 134801 (2012).
14. A. P. Serebrov, A. Fomin, M. S. Onegin, et. al., Tech. Phys. Lett. 40, 10 (2014)
15. J. Martin, B. Franke, K. Hatanaka, S. Kawasaki, and R. Picker, Nucl. Phys. News 31, 19 (2021).
16. S. Sidhu, W. Schreyer, S. Vanbergen, et. al., Eur. Phys.: Web. Conf. (2022) (To be published)
17. S. Ahmed, T. Andalib, M. Barnes et al., Nucl. Instr. Meth. A 927, 101 (2019)
18. M. Kawai, K. Kikuchi, H. Kurishita, et. al., J. Nucl. Mats. 296, 312-320 (2001)
19. A. T. Nelson, J. A. O'Toole, R. A. Valicenti, S. A. Maloy, J. Nucl. Mats. 431, 172-184 (2012).
20. A. Dey, L. Jones, J. Nucl. Mats. 506, 63-70 (2018).
21. R. Garoby et. al. Phys. Scr. 93, 014001 (2018).
22. Los Alamos Scientific Laboratory. Group X-6. (1979)
23. M. Kawai, private communication.
24. T. T. Bohlen, F. Cerutti, M. P. W. Chin, et. al., Nucl. Data Sheets 120, 211-214 (2014)
25. A. Ferrari, P.R. Sala, A. Fasso, J. Ranft, CERN-2005-10 (2005) INFN/TC_05/11, SLAC-R-733
26. S. Saito, K. Suzuki, H. Obata, and Y. Dai, Nucl. Mat. Energy 34, 101338 (2023)
27. Y. Masuda, T. Kitagaki, K. Hatanaka, et. al., Phys. Rev. Lett. 89, 284801 (2002)
28. S. Ahmed, E. Altiere, T. Andalib, et al., Phys. Rev. C 99, 025503 (2019)
29. S. Ahmed, E. Altiere, T. Andalib, et al., Phys. Rev. Accel. Beams 22, 102401 (2019)
30. W. Schreyer, T. Kikawa, M.J. Losekamm, S. Paul, R. Picker, Nucl. Instr. Meth. A 858, 123-129 (2017)
31. W. Schreyer, C. A. Davis, S. Kawasaki, et. al. Nucl. Instr. Meth. A 959, 163525 (2020)